doi: 10.15407/ujpe60.09.0910

N.I. LEBOVKA,[1] L.A. BULAVIN,[2] I.A. MELNYK,[2] K.F. REPNIN,[2] V.I. KOVALCHUK[2]

[1] F.D. Ovcharenko Biocolloidal Chemistry Institute, Nat. Acad. of Sci. of Ukraine
(42, Academician Vernadsky Blvd., Kyiv 03142, Ukraine; e-mail: lebovka@gmail.com)
[2] Taras Shevchenko National University of Kyiv, Faculty of Physics
(2, Academician Glushkov Prosp., Kyiv 03022, Ukraine)

IMPACT OF AGGREGATION ON THE PERCOLATION ANISOTROPY ON A SQUARE LATTICE IN AN ELONGATED GEOMETRY

PACS 47.57.J, 81.40.Cd

The Monte Carlo simulation is applied to study the impact of the aggregation on the percolation anisotropy on a square lattice in the elongated $L_x \times L_y$ geometry. An interactive cluster-growth model, in which the probability of occupying a site on a lattice f_z is dependent on the number of occupied neighboring sites z is used. The value of f_z is $1/r$ at $z = 0$ and is equal to 1 in other cases. The degree of the aggregation parameter $r \geq 1$ controls the morphology of aggregates. The transition from $r = 1$ to $r \to \infty$ corresponds to the transition from the ordinary random percolation to the percolation of compact Eden clusters. The effects of the lattice aspect ratio $a = L_x/L_y$ ($L_x > L_y$) on the finite-size scaling and the electrical conductivity are studied. The data evidence that the percolation threshold p_c goes through the minimum, and the finite-size effects are enhanced with increase in r. The dependence of the electrical conductivity on the measuring direction (x or y) at different values of r and a is discussed.

K e y w o r d s: aggregation, anisotropy, correlated percolation, elongated systems, electrical conductivity.

1. Introduction

The percolation transition reflects changes in the geometrical connectivity of a system, and, commonly, it is accompanied by abrupt changes of different physical characteristics [1]. Nowadays, the percolation phenomena attract a great practical interest stimulated by the necessity to predict electrophysical, thermal, magnetic, and optical properties of various composite systems filled with nanoparticles [2]. In the classical random percolation problem, the filling of the system with particles assumes no presence of correlations. In the correlated percolation problem, the presence of near-neighbors and the interaction between particles are assumed [3, 4]. In the general case, the percolation threshold p_c can depend on the interparticle interactions in a complex way. Up-to-day, the different lattice interactive percolation models, in which the probability of occupying a site f_z is dependent on the number of occupied the neighboring sites z, were proposed [5–9]. For example, in the model of multiplicative growth on a two-dimensional (2d) square lattice, the value of f_z was defined as [5]

$$f_z = (1/r)^{4-z}, \tag{1}$$

where $z \leq 4$ is the number of occupied neighboring sites, and $r \geq 1$ is a degree of aggregation. For this model, $f_z = 1$ at $z = 4$ and $f_z < 1$ at $z < 4$.

In another percolation model of interactive cluster-growth [7–10], it is assumed that the value of f_z is only determined by the presence of neighboring sites:

$$f_z = 1 \text{ at } z \neq 0, \text{ and} \tag{2}$$

$$f_z = 1/r \text{ at } z = 0. \tag{3}$$

The deposition can be considered as a combination of nucleation, growth, and possible coalescence of clusters. For the percolation models of interactive cluster-growth, the value of $r = 1$ corresponds to the ordinary random percolation. The percolation threshold p_c initially decreases and then increases with increasing the degree of aggregation r [10]. For large r ($\gg 1$), the growth of compact Eden clusters was observed. At the percolation threshold, these clusters consolidate into a large percolation cluster [9]. It

was assumed that, in the limit $r \to \infty$, the percolation cluster has a disk-like shape with the percolation threshold $p_c \approx \pi/4 \approx 0.76$ [5]. This value is close to that for equal-sized disks homogeneously distributed on the plane substrate, $p_c = 0.718 \pm 0.003$ [11].

Other correlated percolation models were studied in [12–15]. In a $2d$ correlated percolation model, the attractive interactions between near-neighbor occupied sites result in the formation of a structure reminiscent of discontinuous metal films [12]. In the thermal model of correlated deposition, the occupation of a given site depends on the occupation states of its nearest neighbors, as well as on the temperature [13]. In the granular correlated percolation model, the initial seeds are deposited on the substrate, and the grains are growing around them [14]. The correlated percolation for the deposition on a heterogeneous substrate with two types of sites with different energies of attraction was studied in [15].

Percolation problems for the anisotropic (elongated) geometry have attracted much attention in recent years. The simulation data on the deposition of a mixture of conducting and isolating particles on a $2d$ substrate evidence that the height of the percolation layer is dependent on the concentration of conductive particles p [16]. The crossover between the $2d$ and three-dimensional (3d) percolations on a cubic lattice of the $L_x \times L_y \times L_z$ geometry ($L_x = L_y$) was studied numerically in [17, 18]. For the thickness dependence of the percolation threshold $p_c(L_z)$, the power law behavior at $L_z < 0.1L_x$ is observed

$$p_c(L_z) - p_c^{\infty} \propto L_z^{1/\nu}, \tag{4}$$

where $\nu \approx 0.88$ is a correlation length exponent for the $3d$ percolation problem. However, at $L_z \geq 0.1L_x$, the correction to the scaling is required.

This scaling law is in good correspondence with experimental data on the thickness dependence of the percolation threshold of an Al–Ge film [19].

Simulations of the continuum percolation in $3d$ rectangular samples filled with spherical particles were done in [20]. The findings indicate that the sample shape and the relative sizes influence the percolation behavior. The critical volume fraction p_c across the thin direction of the film is lower than the classical limit of $\approx$0.29 (for spheres in a $3d$ matrix) and increases with the film thickness. The $2d$-3d percolation transition for a system composed of equisized, fully penetrable ellipsoids was numerically investigated in [21]. The percolation threshold is significantly dependent upon the preferential orientation of particles.

The $2d$ rectangular $L_x \times L_y$ geometry was investigated extensively in [22–34]. The aspect ration was determined as $a = L_x/L_y \geq 1$. For the ordinary random percolation, the growth of percolation clusters was observed dominantly along the short axis L_y (easy direction for percolation), whereas the percolation in the direction of the long axis L_x (a difficult direction for percolation) was observed infrequently. The different finite-size scaling functions were derived for the percolation threshold dependences p_c^x and p_c^y [22–24, 30, 34].

The 1d-2d percolation transition in a $L_x \times L_y$ strip for the model of nodes and links was analyzed in [22, 23]. It was demonstrated that the 1d effects became important for the large strip length,

$$L_x > L_y \exp(L_y/\xi)^{d_f}, \tag{5}$$

where $\xi \propto (p - p_c)^{-\nu}$ is a correlation length for the $2d$ percolation problem, $\nu = 4/3$ is a correlation length exponent, and $d_f \approx 1.56$ is a fractal dimensionality of very large clusters below the percolation threshold.

For an apparent percolation threshold (the value of p_c, when 50% of realizations are percolating), the following scaling laws were conjectured [34]:

$$p_c^x - p_c^{\infty} = \Lambda(a)(L_x)^{-1/\nu}, \tag{6}$$

$$p_c^y - p_c^{\infty} = -\Lambda(a)(L_x)^{-1/\nu}, \tag{7}$$

where $\Lambda(a) = c(a^{-1/\nu} - 1)$, c ($=0.92 \pm 0.04$) is a constant, p_c^{∞} ($\approx$0.59275) is the infinite system-size percolation threshold for the site percolation, and ν ($=4/3$) is a correlation length exponent for a $2d$ system.

A scaling theory was used to study the $3d$ to $2d$ transition near the percolation threshold for an $L_x \times L_y \times L_z$ ($L_x = L_y \gg L_z$) system [35]. The percolation threshold p_z in the direction z is dependent upon the thickness of the layer L_z with the transition from $p_c^{2d} = 0.59275$ for a $2d$ system ($L_z = 1$) to $p_c^{3d} = 0.3117$ for a $3d$ system ($L_z = \infty$). The following scaling relation was obtained for p_z versus L_z dependence:

$$p_c^z = p_c^{3d} + (p_c^{2d} - p_c^{3d})L^{-1/\nu}, \tag{8}$$

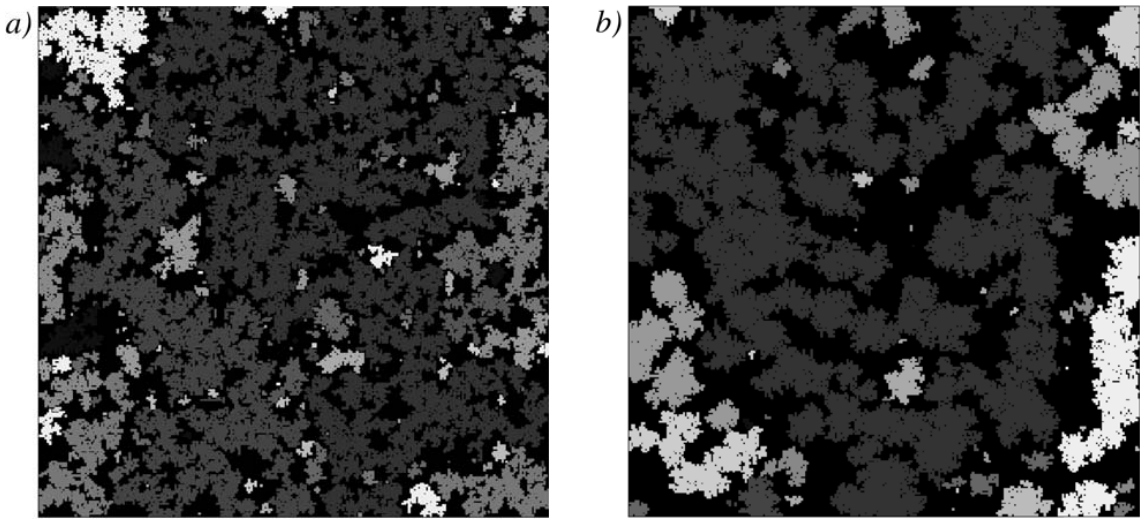

Fig. 1. Examples of growth patterns in a vicinity of the percolation thresholds for $p = 0.52$ and $r = 100$ (a) and $p = 0.55$ and $r = 1000$ (b). The data are presented for the square system $L_x = L_y = 256$. The black color corresponds to the empty sites

where $\nu = 0.88$ is a correlation length exponent for the $3d$ percolation problem.

Effects of anisotropy on the electrical conductivity in finite rectangular lattices were studied as well (see [19, 32, 33, 36]). The electrical conductivity as a function of the film (Al-Ge random mixture) thickness L_z was experimentally measured in [19]. The system behaves itself as a $3d$ system, when the film thickness L_z is much larger than the correlation length. For the model of deposition of conducting particles on a $2d$ substrate, the following scaling law for the thickness dependence of the electrical conductivity $\sigma(L_z)$ was derived [36]:

$$\sigma \propto (L_z - L_z^c)^t, \tag{9}$$

where t is the critical conductivity exponent, and L_z^c is the critical thickness.

The data of experiments and simulations [32] for the deposition of particles on a substrate evidence that the percolation threshold is shifted to extremely low surface coverages. The transfer matrix method was applied to calculate the electrical conductivity along the short direction y for $L_y = 10$ and for various values of L_x in the interval $1 \div 1000$ [33]. The conductance jump was observed at some critical value of L_x, and its position was dependent on the fraction of occupied sites p. The electrical conductivity in finite rectangular random resistor networks as a function of the geometrical aspect ratio a was simulated in [37]. A numerical resistor network model on a cubic lattice of $L_x \times L_y \times L_z$ geometry ($L_x = L_y$) [18] predicts the following dependence on L_z/L_x for the conductivity exponent t:

$$t - t_{2d} \propto L_z/L_x, \text{at } L_z < 0.1L_x \text{ and} \tag{10}$$

$$t - t_{2d} \propto \ln(L_z/L_x), \text{at } L_z \geq 0.1L_x. \tag{11}$$

Here, $t_{2d} \approx 4/3$ is the conductivity exponent for $2d$ systems.

This work is aimed to study the impact of the aggregation on the percolation anisotropy on a square lattice in the elongated $L_x \times L_y$ geometry. The interactive cluster-growth model [9], in which the probability of occupying a site on a lattice f_z is dependent on the number of occupied neighboring sites z, is used. The effects of the lattice aspect ratio $a = L_x/L_y$ ($L_x > L_y$) on the finite-size scaling and the electrical conductivity are investigated. The dependences of the electrical conductivity on the directions x and y at various values of r and a are also discussed.

2. Description of the Model and Details of Calculations

The growth of percolation n-clusters is based on the previously described interactive cluster-growth model [9]. The sites of the $2d$ square lattice were sequentially filled, by using the following rules:

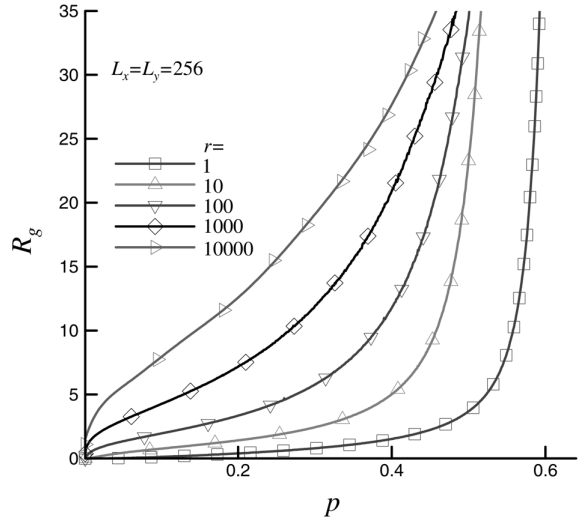

Fig. 2. Mean radius of gyration R_g versus the fraction of occupied sites p for the square system $L_x = L_y = 256$ at various values of the aggregation degree r

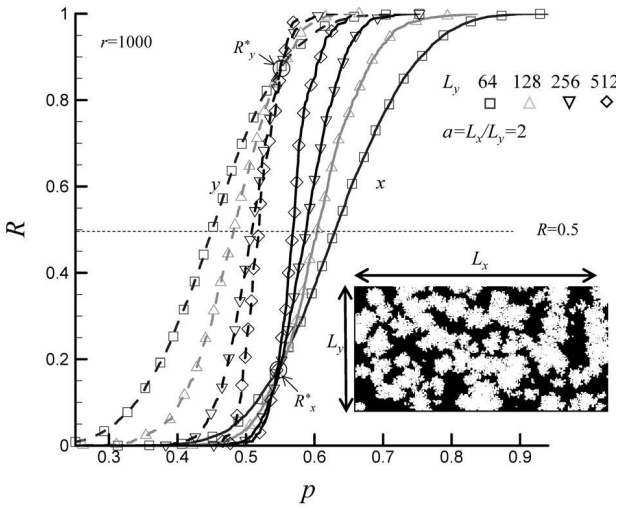

Fig. 3. Percolation probability R versus the fraction of occupied sites p for the different directions x and y at different values of L_y. The aspect ratio is $a = L_x/L_y = 2$ and the aggregation degree is $r = 1000$

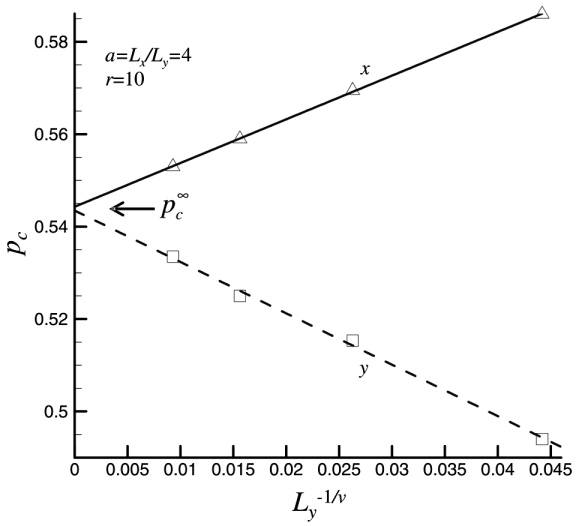

Fig. 4. Apparent percolation threshold p_c versus $L_y^{-1/\nu}$. The aspect ratio is $a = L_x/L_y = 4$, and the aggregation degree $r = 10$. The value of p_c^∞ corresponds to the percolation threshold of an infinite lattice

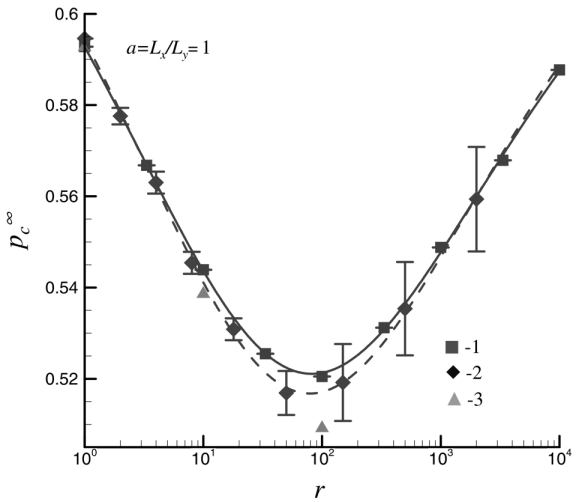

Fig. 5. Percolation threshold p_c^∞ versus the aggregation degree r. Here, symbol 1 corresponds to the data of the present work, symbol 2 to the data of [10], and symbol 3 to the data of [9]

- the new empty site is randomly selected from the list;
- the number of filled nearest neighbors z is determined;
- the site is filled with probability f_z as determined from Eqs. (2) and (3).

The fraction of occupied sites p is determined as the ratio of the number of filled sites and the product L_xL_y. The lattice is filled to a given concentration p and then is checked for the presence of a percolation cluster.

Figure 1 presents the examples of growth patterns in vicinities of the percolation thresholds at various values of aggregation degree r for the square system $L_x = L_y = 256$. The visual analysis of the data shows that an increase of r results in an increase of the mean

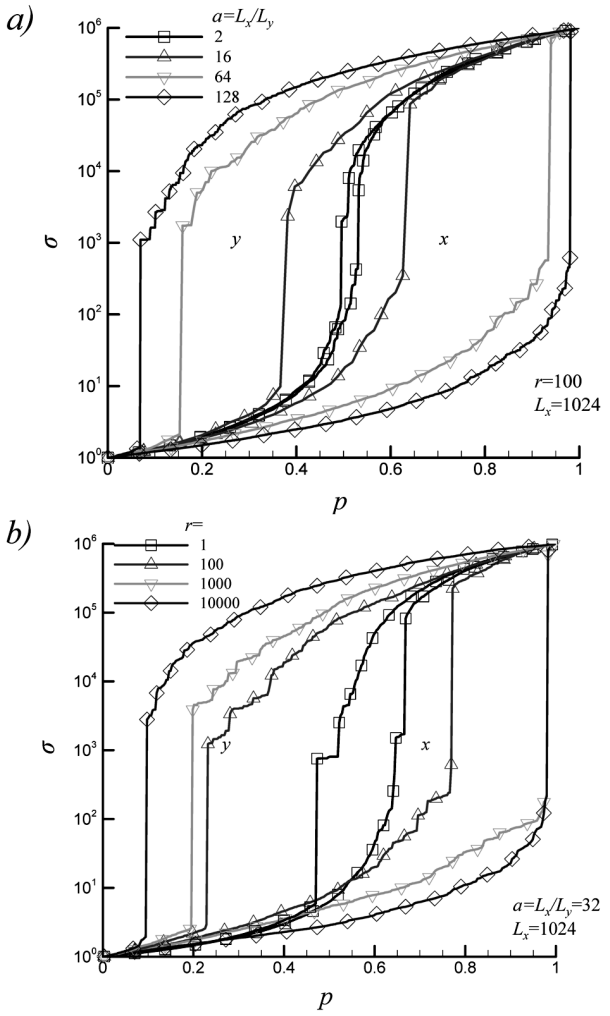

Fig. 6. Examples of the electrical conductivity σ versus the fraction of occupied sites p for the directions x and y at different values of a and $r = 100$ (a) and different values of r and $a = 32$ (b). The long-side size of the square lattice is $L_x = 1024$

cluster size. For the qualitative characterization, the radius of gyration of an individual cluster R_s is calculated as [38]

$$R_s = \sqrt{\frac{1}{s}\sum_{i=1}^{s} |\mathbf{r}_i - \mathbf{r}_o|^2}, \tag{12}$$

where vector $\mathbf{r}_i$ determines the position of the i-th site in the cluster, s is a number of particles in the cluster, and

$$r_o = \frac{1}{s}\sum_{i=1}^{s} \mathbf{r}_i. \tag{13}$$

Figure 2 presents examples of the mean radius of gyration R_g versus the fraction of occupied sites p for the square system $L_x = L_y = 256$ at various values of the aggregation degree r. Note that size of the cluster noticeably increases with r at the fixed value of p.

The investigations were done on the elongated square lattices with various sizes in the horizontal x and vertical y directions: $L_x \geq L_y$. The periodical boundary conditions were used in the both x and y directions.

The Hoshen–Kopelman algorithm was used for the labeling of different clusters [39]. The value of percolation threshold p_c corresponds to the minimum fraction of occupied sites, at which an infinite cluster formed in the infinite lattice. For the estimation of p_c, the percolation probability R versus the fraction of occupied sites p was calculated. The long lattice side was varied in the interval of $L_x = 64$–2048, and the number of runs was up to 1000.

The electrical conductivity of the system is calculated, by using the highly efficient algorithm proposed by Frank and Lobb [40]. This algorithm utilizes the repeated application of a sequence of series, parallel, and star-triangle (Y–△) transformations to the lattice bonds. The final result of this sequence of transformations is the reduction of a finite portion of the lattice to a single bond that has the same conductance as the entire lattice portion. We used the scheme of four equivalent resistors (see, e.g. [41]) with high, $\sigma_f = 10^6$, and low, $\sigma_i = 1$, conductivities for the occupied and empty sites, respectively.

3. Results and Discussion

Figure 3 presents examples of the percolation probability R versus the fraction of occupied sites p for the different directions x and y at different values of L_y. For finite-sized systems, the probability curves $R(p)$ for fixed values of L_z and a evidence that the dominant growth of percolation clusters occurs initially in the direction of the short axis y (easy direction for percolation) and then in the direction of the long axis x (difficult direction for percolation). It is in full correspondence with a similar behavior observed for the ordinary random percolation problem [22–31, 33, 34]. All curves $R(p)$ for different L_z cross each other at a unique intersection point $R_x^* = R_y^*$ located at $p_c = p_c^\infty$ in the thermodynamic limit.

The apparent percolation threshold p_c at a given lattice size $L_x \times L_y$ is determined in the directions x

and y. The condition $R(p) = 0.5$ (i.e., when 50% of realizations are percolating) is used [42]. The finite-size scaling analysis was done to obtain the percolation threshold in the thermodynamic limit, at $L_x \to \infty$ and $L_y \to \infty$. The percolation threshold p_c^∞ of an infinite lattice can be found by fitting the results obtained for lattices of different sizes to the scaling laws described by Eqs. (6) and (8). The example of such fitting is presented in Fig. 4.

Note that, at the relatively large values of $r > 100$, the noticeable violations of the scaling laws described by Eqs. (6) and (8) are observed for the studied interval of $L_x = 64$–2048, and the apparent values of p_c noticeably deviate from their magnitude in the thermodynamic limit. Figure 5 presents the percolation threshold p_c^∞ versus the aggregation degree r. The value of p_c^∞ initially decreases, goes through the minimum at $r \approx 10^2$, and then increases with r. For the finite systems, the apparent anisotropy of the percolation $p_c^x - p_c^y$ increases with r.

Figure 6 presents examples of the electrical conductivity σ versus the fraction of occupied sites p for the different direction x and y at different values of a and $r = 100$ (a) and different values of r and $a = 32$ (b). The value of σ jumps in a vicinity of the percolation threshold p_c. In addition, the strong anisotropy of the electrical conductivity is observed, and the value of σ_y exceeds the value of σ_x.

The anisotropy of the electrical conductivity increased with the values of r (Fig. 6, a) and a (Fig. 6, b). The apparent percolation threshold in the short direction $p_c^y(a)$ can be noticeably smaller than that $p_c^x(a)$ in the long direction, and $p_c^y(a) < p_c^y(a = 1) < p_c^y(a)$, where $p_c^y(a = 1)$ is the apparent percolation threshold for the isotropic lattice.

The further investigations of the scaling of the electrical conductivity anisotropy with regard for the geometrical arguments is in progress and will allow one to clarify the conduction mechanisms of thin film nanomaterials for potential applications in optoelectronics and sensors.

4. Conclusions

The impact of the aggregation on the percolation anisotropy for a square lattice in the elongated $L_x \times L_y$ geometry is studied. The aggregation is simulated, by using an interactive cluster-growth model, in which the degree of aggregation is controlled by the parameter $r \geq 1$. The transition from $r = 1$ to $r \to \infty$ corresponds to the transition from the ordinary random percolation to the percolation of compact Eden clusters. The data evidence that the percolation threshold p_c goes through the minimum, and the finite-size effects are enhanced with increasing r. For elongated systems, the electrical conductivities are strongly dependent upon the direction of measurements, and the apparent percolation threshold in the short direction $p_c^y(a)$ is noticeably smaller than that, $p_c^x(a)$, in the long direction. The obtained data may be useful for understanding the electro-physical behavior of composite films filled with nanoparticles that have tendency to the agglomeration and aggregation.

The authors would like to acknowledge the partial financial support of project 43-02-15(U), Ukraine (N.L.).

1. D. Stauffer, in *Quantum and Semi-Classical Percolation and Breakdown in Disordered Solids* (Springer, Berlin, 2009), p. 1.
2. S. De and J. Coleman, MRS Bulletin **36**, 774 (2011).
3. A. Weinrib, Phys. Rev. B **29**, 387 (1984).
4. S. Safran, I. Webman, and G. Grest, Phys. Rev. A **32**, 506 (1985).
5. L. Duckers and R. Ross, Phys. Lett. A **49**, 361 (1974).
6. L. Duckers, Phys. Lett. A **67**, 93 (1978).
7. J.W. Evans, J.A. Bartz, and D.E. Sanders, Phys. Rev. A **34**, 1434 (1986).
8. D. Sanders and J. Evans, Phys. Rev. A **38**, 4186 (1988).
9. S.R. Anderson and F. Family, Phys. Rev. A **38**, 4198 (1988).
10. J.W. Evans, J. Phys. A **23**, L197 (1990).
11. E.T. Gawlinski and H.E. Stanley, J. Phys. A **14**, L291 (1981).
12. D. Wollman, M. Dubson, and Q. Zhu, Phys. Rev. B **48**, 3713 (1993).
13. A. Sadiq and M. Khan, Z. Phys. B **39**, 131 (1980).
14. T. Odagaki, H. Kawai, and S. Toyofuku, Physica A **266**, 49 (1999).
15. M. Gimenez, A. Ramirez-Pastor, and F. Nieto, Physica A **389**, 1521 (2010).
16. N.I. Lebovka, S.S. Manna, S. Tarafdar, and N. Teslenko, Phys. Rev. E **66**, 066134 (2002).
17. P. Sotta and D. Long, Eur. Phys. J. E **11**, 375 (2003).
18. L. Zekri, A. Kaiss, J.-P. Clerc, B. Porterie, and N. Zekri, Phys. Lett. A **375**, 346 (2011).
19. A. Kapitulnik and G. Deutscher, J. Phys. A **16**, 2889 (1983).
20. D.R. Stevens, E.W. Skau, L.N. Downen, M.P. Roman, and L.I. Clarke, Phys. Rev. E **84**, 021126 (2011).

21. Y.-B. Yi, C.-W. Wang, and A.M. Sastrya, J. Electrochem. Soc. **151**, A1292 (2004).
22. G. Deutscher, Phys. Rev. B **25**, 490 (1982).
23. Y. Gefen, Y. Kantor, and G. Deutscher, J. Phys. A **15**, L553 (1982).
24. R. Monetti and E. Albano, Z. Phys. B **82**, 129 (1991).
25. R. Monetti and E. Albano, Z. Phys. **90**, 351 (1993).
26. R. Monetti and E. Albano, J. Phys. A **26(16)**, 3955 (1993).
27. R.A. Monetti and E.V. Albano, Phys. Rev. E **49**, 199 (1994).
28. H.-P. Hsu, S.C. Lin, and C.-K. Hu, Phys. Rev. E **64**, 016127 (2001).
29. S.J. Marrink and M.A. Knackstedt, J. Phys. A **32**, L461 (1999).
30. S.J. Marrink and M.A. Knackstedt, Phys. Rev. E **62**, 3205 (2000).
31. S. Tsubakihara, Phys. Rev. E **62**, 8811 (2000).
32. J. Schmelzer, S.A. Brown, A. Wurl, M. Hyslop, and R.J. Blaikie, Phys. Rev. Lett. **88**, 226802 (2002).
33. E. Meilikhov, Phys. Lett. A **346**, 193 (2005).
34. M. Masihi, P.R. King, and P. Nurafza, Phys. Rev. **74**, 42102 (2006).
35. A.V. Neimark, Zh. Eksp. Teor. Fiz. **98**, 611 (1990).
36. M. Nakamura, J. Non-Cryst. Sol. **849**, 156158 (1993).
37. T. Kiefer, G. Villanueva, and J. Brugger, Phys. Rev. E **80**, 21104 (2009).
38. L.A. Bulavin, N.V. Vygornitskii, and N.I. Lebovka, *Computer Simulation of Physical Systems* (Intellect, Dolgoprudnyi, 2011) (in Russian).
39. D. Stauffer and A. Aharony, *Introduction to Percolation Theory* (Taylor & Francis, Boca Raton, 1992).
40. D.J. Frank and C.J. Lobb, Phys. Rev. B **37**, 302 (1988).
41. V.A. Cherkasova, Y.Y. Tarasevich, N.I. Lebovka, and N.V. Vygornitskii, Eur. Phys. J. B **74**, 205 (2010).
42. R.M. Ziff and M.E.J. Newman, Phys. Rev. E **66**, 016129 (2002).

Received 29.05.15

М.І. Лебовка, Л.А. Булавін,
І.А. Мельник, К.Ф. Реппін, В.І. Ковальчук

ВПЛИВ АГРЕГАЦІЇ НА АНІЗОТРОПІЮ ПЕРКОЛЯЦІЇ НА КВАДРАТНІЙ ҐРАТЦІ В ПОДОВЖЕНІЙ ГЕОМЕТРІЇ

Р е з ю м е

Метод Монте-Карло був застосований для вивчення впливу агрегації на анізотропію перколяції на квадратній ґратці в подовженій $L_x \times L_y$ геометрії. Була використана модель взаємодіючої перколяції, в якій імовірність зайняття певного вузла кластера на ґратці f_z залежить від числа зайнятих сусідніх вузлів z. Величина f_z дорівнювала $1/r$ при $z = 0$ або дорівнювала 1 в інших випадках. Параметр ступеня $r \geq 1$ контролює морфологію агрегатів. Перехід від $r = 1$ до $r \to \infty$ відповідає переходу від звичайної випадкової перколяції до перколяції по компактним кластерам Ідена. Вивчено вплив аспектного відношення сторін ґратки $a = L_x/L_y$ $(L_x > L_y)$ на скінченно-вимірний скейлінг і поведінку електропровідності. Отримані дані свідчать, що поріг перколяції p_c проходить через мінімум і скінченно вимірні ефекти підсилюються при збільшенні r. Обговорюються залежності електропровідності від напрямку вимірювання при різних значеннях r і a.